Two-Loop Corrections to the Decay Rate of Orthopositronium

G.S. Adkins[1], R.N. Fell[2], and J. Sapirstein[3]

[1] Franklin & Marshall College, Lancaster PA 17604, USA
[2] Brandeis University, Waltham MA 02254, USA
[3] University of Notre Dame, Notre Dame IN 46556, USA

Abstract. Order α^2 corrections to the decay rate of orthopositronium are calculated in the framework of nonrelativistic QED. The correction is ≈ 45 in units of $(\alpha/\pi)^2$ times the lowest order rate.

1 Introduction

The theoretical result for the orthopositronium decay rate is

$$\Gamma(\text{theory}) = \Big\{1 + A\frac{\alpha}{\pi} + \frac{\alpha^2}{3}\ln\alpha + B\Big(\frac{\alpha}{\pi}\Big)^2 - \frac{3\alpha^3}{2\pi}\ln^2\alpha + C\frac{\alpha^3}{\pi}\ln\alpha + D\Big(\frac{\alpha}{\pi}\Big)^3 + \cdots\Big\}\Gamma_0 \tag{1}$$

where

$$\Gamma_0 = \frac{2}{9}(\pi^2 - 9)\frac{m\alpha^6}{\pi} = 7.2111670(1)\,\mu s^{-1} \tag{2}$$

is the Ore and Powell result for the lowest order decay rate [1,2], and

$$A = -10.286606(10) \tag{3}$$

is the order α correction [3,4,5]. The $\alpha^2\ln\alpha$ logarithmic contribution with coefficient $1/3$ was obtained in 1979 [6], and the $\alpha^3\ln^2\alpha$ logarithmic contribution with coefficient $-3/(2\pi)$ in 1993 [7]. The $(\alpha/\pi)^2$ correction has two parts: from decay to five photons [0.187(11)] [8,9], and from decay to three photons. Our new result is the three photon decay contribution: 44.86(26) [10]. Finally, the coefficient of the $(\alpha^3/\pi)\ln\alpha$ contribution has recently been obtained by three groups: $C = A/3 - 229/30 + 8\ln 2 = -5.517$ [11,12,13].

Numerical values for the various contributions to the decay rate are shown in Table 1. In looking at this table, one should keep in mind the approximate value of the current experimental uncertainty for this rate, which is $\approx 0.002\,\mu s^{-1}$ (see Table 2). It seems clear that the perturbation series is behaving nicely, and that "higher-order" terms are indeed small. For example, the ratios of the $O(\alpha)$ to $O(1)$ terms and the $O(\alpha^2)$ to $O(\alpha)$ terms are

$$|A/1|\frac{\alpha}{\pi} = 0.023\,, \tag{4}$$

$$|B/A|\frac{\alpha}{\pi} = 0.010\,. \tag{5}$$

Table 1. Numerical values of contributions to the orthopositronium decay rate

term	contribution (in μs^{-1})
1	7.211167
$A\frac{\alpha}{\pi}$	-0.172303
$\frac{\alpha^2}{3}\ln\alpha$	-0.000630
$B\left(\frac{\alpha}{\pi}\right)^2$	0.001753(11)
$-\frac{3\alpha^3}{2\pi}\ln^2\alpha$	-0.000032
$C\frac{\alpha^3}{\pi}\ln\alpha$	0.000024
$D\left(\frac{\alpha}{\pi}\right)^3$	0.00000009 D
total	7.039979(11) + 0.00000009D

If the unknown D contribution follows roughly the same pattern, and $|D/B|\alpha/\pi = 0.010$, then one would have $D = 192$ and its contribution would be $D(\alpha/\pi)^3\Gamma_0 = 0.000017\ \mu s^{-1}$. If D were 10 times this large, its contribution would still be much smaller than the present experimental uncertainty.

Our final result is

$$\Gamma(\text{theory}) = 7.039979(11)\ \mu s^{-1}\ . \tag{6}$$

We have not assigned a theoretical error to the uncalculated D term, but note that D would have to be about 20000 for this contribution to be as large as the experimental error.

The theoretical result is significantly below the two Michigan experimental values [14,15], but is in agreement with the lower precision Tokyo experimental value [16] (see Table 2).

Table 2. Recent experimental results for the orthopositronium decay rate. The quantity Δ is the difference between the experimental and theoretical values for the rate in terms of the experimental uncertainty σ

medium	place	year	result (in μs^{-1})	Δ	reference
gas	Michigan	1989	7.0514(14)[a]	8.1 σ	[14]
vacuum	Michigan	1990	7.0482(16)	5.1 σ	[15]
powder	Tokyo	1995	7.0398(29)	-0.1 σ	[16]

[a] At this meeting, Ralph Conti announced that the value of the Michigan gas number will be corrected to bring its value down closer to the vacuum result [17].

2 NRQED

We use nonrelativistic QED (NRQED) [18] as the framework for this calculation. In particular, we use an implementation similar to that used by Hoang, Labelle, and Zebarjad [19,20] in their calculation of the two-loop corrected one-photon-annihilation contribution to the positronium hyperfine structure. Their calculation and ours are very closely related: theirs involves the virtual decay of orthopositronium to a single photon, while ours involves the real decay of orthopositronium to three photons. However, there are substantial differences between three-photon real decay and one-photon virtual decay. In three-photon decay the photons go off in unspecified directions in a plane which brings in the need to integrate over two parameters which describe the configuration of the decay. The three-photon graphs are considerably more complicated than the one-photon graphs because of the increased number of real and virtual particles. There are many more graphs to be considered (83 *vs.* 6) in the decay rate calculation. And finally, in three-photon real decay the energy-shift graphs have imaginary parts which are related to the decay rate.

The implementation of NRQED used here is defined by the Lagrangian and the treatment of infrared and ultraviolet divergences. The Lagrangian has the form [20,21]

$$\begin{aligned}
\mathcal{L}_{\rm NRQED} = {} & \frac{1}{2}(\boldsymbol{E}^2 - \boldsymbol{B}^2) \\
& + \psi^\dagger \Big[\mathrm{i}D_t + \frac{\boldsymbol{D}^2}{2m} + \frac{\boldsymbol{D}^4}{8m^3} + \cdots + \frac{c_F e}{2m} \boldsymbol{\sigma} \cdot \boldsymbol{B} \\
& + \frac{c_D e}{8m^2} (\boldsymbol{D} \cdot \boldsymbol{E} - \boldsymbol{E} \cdot \boldsymbol{B}) + \frac{c_S e}{8m^2} \mathrm{i} \boldsymbol{\sigma} \cdot (\boldsymbol{D} \times \boldsymbol{E} - \boldsymbol{E} \times \boldsymbol{D}) + \cdots \Big] \psi \\
& + (\psi \to \chi) \\
& - \frac{d_C e^2}{4m^2} (\psi^\dagger \boldsymbol{\sigma} \sigma_2 \chi^*) \cdot (\chi^T \sigma_2 \boldsymbol{\sigma} \psi) \\
& + \frac{d_D e^2}{3m^4} \frac{1}{2} \big[(\psi^\dagger \boldsymbol{\sigma} \sigma_2 \chi^*) (\chi^T \sigma_2 \boldsymbol{\sigma} (-\mathrm{i} \overleftrightarrow{\boldsymbol{D}}/2)^2 \psi) + \mathrm{H.C.} \big] + \cdots
\end{aligned} \tag{7}$$

where ψ and χ are the two-component electron and positron fields, $D_t = \partial_t - \mathrm{i}eA_0$, $\boldsymbol{D} = \boldsymbol{\nabla} + \mathrm{i}e\boldsymbol{A}$, and $\boldsymbol{\sigma}^i$ is the usual Pauli matrix. The Fermi, Darwin, spin-orbit, and the four-fermion contact and derivative couplings c_F, c_D, c_S, d_C, and d_D all have the form $1 + O(\alpha)$ by matching with tree-level QED. Ultraviolet divergences are regulated by a momentum-space cutoff $m\Lambda$, while infrared divergences are controlled by a non-zero photon mass $m\lambda$. We make use of Coulomb gauge, in which the photon propagator has the form $1/D(\boldsymbol{k})$ for Coulomb photons and

$$D_{ij}(k) = \frac{1}{k^2 - \lambda^2 + \mathrm{i}\epsilon} \Big(\delta_{ij} - \frac{k_i k_j}{D(\boldsymbol{k})} \Big) \tag{8}$$

for transverse photons (where $D(\boldsymbol{k}) = \boldsymbol{k}^2 + \lambda^2$). The electron propagator is

$$S(p) = \frac{1}{p_0 - \boldsymbol{p}^2/(2m) + \mathrm{i}\epsilon} \,. \tag{9}$$

In the related calculation of Hoang, Labelle, and Zebarjad [20], ultraviolet divergences were regulated by a momentum-space cutoff as here, but infrared divergences were dealt with by keeping the particles above threshold (to control binding singularities) and also including a non-zero photon mass (to regulate the remaining infrared divergences). In the two-loop parapositronium decay rate calculation of Czarnecki, Melnikov, and Yelkhovsky [22,23], both ultraviolet and infrared divergences were regulated via dimensional regularization. We chose to regulate all infrared and binding singularities by a photon mass in order to make contact with the NRQED work done by Labelle, Lepage, and Magnea [24] on the orthopositronium decay rate problem. A nontrivial check of our implementation of NRQED is provided by making sure that it reproduces the results of Ref. [20], with both NRQED calculations confirmed by an entirely different Bethe-Salpeter type calculation [25].

To the order of interest here the relevant NRQED interactions (see Fig. 1) can be represented as instantaneous potentials [20]. They are

$$V_4(\boldsymbol{p},\boldsymbol{q}) = \frac{2\pi\alpha}{m^2} d_C \,, \tag{10}$$

$$V_{4der}(\boldsymbol{p},\boldsymbol{q}) = -\frac{4\pi\alpha}{3m^4}(\boldsymbol{p}^2+\boldsymbol{q}^2) d_D \,, \tag{11}$$

$$V_{coul}(\boldsymbol{p},\boldsymbol{q}) = -\frac{4\pi\alpha}{D(\boldsymbol{k})} \,, \tag{12}$$

$$\delta H_{kin}(\boldsymbol{p},\boldsymbol{q}) = -(2\pi)^3 \delta(\boldsymbol{p}-\boldsymbol{q}) \frac{q^4}{4m^3} \,, \tag{13}$$

$$V_{BF}(\boldsymbol{p},\boldsymbol{q}) = -\frac{2\pi\alpha}{m^2}\Big\{ \frac{\boldsymbol{p}^2+\boldsymbol{q}^2}{D(\boldsymbol{k})} - \frac{11}{6}\frac{\boldsymbol{k}^2}{D(\boldsymbol{k})} + \frac{\lambda^2(\boldsymbol{p}^2+\boldsymbol{q}^2)}{D^2(\boldsymbol{k})} + \frac{\lambda^4}{2D^2(\boldsymbol{k})} - \frac{\lambda^2}{2D(\boldsymbol{k})} \Big\} \,. \tag{14}$$

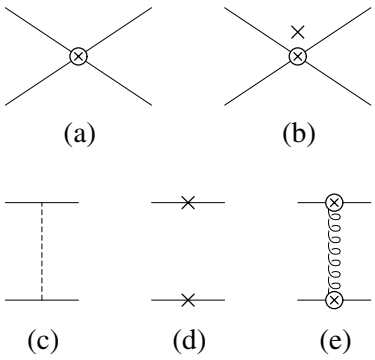

Fig. 1. The NRQED instantaneous potentials: (a) four-fermion contact, (b) four-fermion derivative, (c) Coulomb, (d) relativistic kinetic energy, and (e) Breit-Fermi

The relativistic correction to the fermion kinetic energy is represented as a potential. The Breit-Fermi interaction includes the effects of transverse photon exchange as well as relativistic corrections to Coulomb photon exchange. The potentials are given with the assumption that the states acted on are S states with total spin 1.

3 The Matching Calculation

The next step in the implementation of NRQED is to determine the NRQED coefficients by requiring agreement between NRQED and QED for appropriately chosen scattering amplitudes. Of particular interest for the decay rate calculation are the four-fermion coefficients d_C and d_D, which encode the effects of decay in their imaginary parts. The scattering process we will discuss is $e^-e^+ \to e^-e^+$ scattering at threshold in the total spin 1 configuration. On the QED side, the two graphs of Fig. 2a and Fig. 2b represent the leading contributions to the real and imaginary parts of d_C and d_D. We will work in terms of energy shifts and decay rate contributions by defining

$$\Delta E = \mathrm{i}(\text{amplitude}) \times \phi_0^2 \,, \tag{15}$$

$$\Gamma \quad = -2\mathrm{Im}(\Delta E) \,, \tag{16}$$

where $\phi_0^2 = m^3\alpha^3/(8\pi)$ is the square of the nonrelativistic Coulomb ground state wave function at the origin. Then the energy shift and decay rate described by Fig. 2a and Fig. 2b are

$$\Delta E = \frac{m\alpha^4}{4} \,, \tag{17}$$

$$\Gamma \quad = \Gamma_0 = \frac{2}{9}(\pi^2 - 9)\frac{m\alpha^6}{\pi} \,. \tag{18}$$

The corresponding energy and rate from Fig. 1a and Fig. 1b are

$$\Delta E = \frac{2\pi\alpha}{m^2}\mathrm{Re}(d_C)\phi_0^2 = \frac{m\alpha^4}{4}\mathrm{Re}(d_C) \,, \tag{19}$$

$$\Gamma \quad = -\frac{m\alpha^4}{2}\mathrm{Im}(d_C) \,. \tag{20}$$

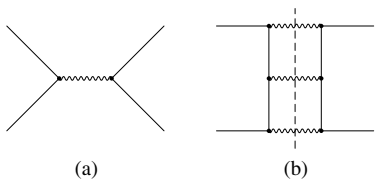

Fig. 2. QED graphs contributing to the lowest order energy shift and decay rate. The dashed vertical line represents a Cutkosky cut through the three-photon intermediate state used to find the imaginary part

Tree-level matching then gives

$$\mathrm{Re}(d_C) = 1 + O(\alpha) \,, \tag{21}$$

$$\mathrm{Im}(d_C) = -\frac{4(\pi^2-9)\alpha^2}{9\pi} + O(\alpha^3) \,. \tag{22}$$

If we write

$$\mathrm{Im}(d_C) = -\frac{4(\pi^2-9)\alpha^2}{9\pi} e \tag{23}$$

where

$$e = 1 + (\alpha/\pi)e_1 + (\alpha/\pi)^2 e_2 + \cdots \tag{24}$$

then we will need to evaluate e up through terms of order α^2.

Similarly, the real and imaginary parts of d_D are found by considering the same QED graphs Fig. 2a and Fig. 2b slightly above threshold. One finds that [26,24]

$$\mathrm{Re}(d_D) = 1 + O(\alpha) \,, \tag{25}$$

$$\mathrm{Im}(d_D) = -\frac{(\pi^2-9)X\alpha^2}{36\pi} \,, \tag{26}$$

where $X = (19\pi^2 - 132)/(\pi^2 - 9)$.

Now we proceed to the one- and two-loop calculations in QED and NRQED.

The graphs contributing the orthopositronium decay at one-loop order in QED are shown in Fig. 3. The one-loop graphs contribute [10]

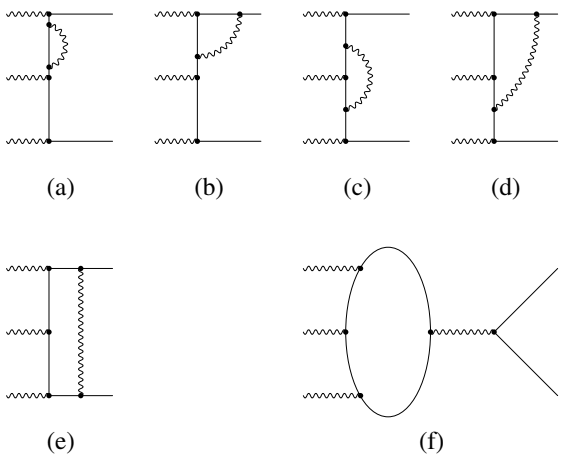

Fig. 3. One-loop QED graphs contributing to the orthopositronium decay rate. They are (a) the self-energy graph, (b) the outer vertex graph, (c) the inner vertex graph, (d) the double vertex graph, (e) the ladder graph, and (f) the annihilation graph

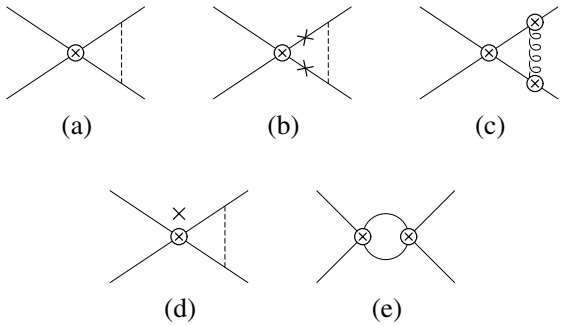

Fig. 4. One-loop NRQED graphs contributing to the orthopositronium decay rate

$$\Gamma_1^{\rm QED} = \big[\frac{2\pi}{\lambda} + A(\lambda)\big]\frac{\alpha}{\pi}\Gamma_0 \tag{27}$$

where

$$A(\lambda) = -10.286606(10) + 15.39\,\lambda\,. \tag{28}$$

Even though the limit $\lambda \to 0$ is taken at the end of the calculation, we keep terms of order λ in the one-loop calculation because terms with a factor of $1/\lambda$ enter at the two-loop order. The NRQED one-loop graphs are shown in Fig. 4, and their values are given in Table 3. The matching condition through one-loop order is thus

$$\begin{aligned} &1 + \frac{\alpha}{\pi}\big[\frac{2\pi}{\lambda} + A(\lambda)\big] \\ &\quad = \big[1 + \frac{\alpha}{\pi}e_1\big] + \frac{\alpha}{\pi}\big[\frac{2\pi}{\lambda} + \big(-\frac{8}{3} - \frac{X}{6}\big)\Lambda + \big(\frac{7}{12} + \frac{X}{12}\big)\pi\lambda\big]\,, \end{aligned} \tag{29}$$

Table 3. One-loop NRQED decay rate contributions

diagram	$\frac{\alpha}{\lambda}\Gamma_0$	$\frac{\alpha\Lambda}{\pi}\Gamma_0$	$\alpha\lambda\Gamma_0$
a	$2e$	0	0
b	0	1	$-\frac{1}{2}$
c	0	$-\frac{5}{3}$	$\frac{13}{12}$
d	0	$-\frac{X}{6}$	$\frac{X}{12}$
e	0	-2	0
total	$2e$	$-\frac{8}{3} - \frac{X}{6}$	$\frac{7}{12} + \frac{X}{12}$

where a factor of Γ_0 has been removed from each side. Thus one has

$$e_1 = \big(\frac{8}{3} + \frac{X}{6}\big)\Lambda + A(\lambda) - \big(\frac{7}{12} + \frac{X}{12}\big)\pi\lambda\,. \tag{30}$$

The two-loop calculation is significantly more involved. There are 83 independent two-loop QED graphs that contribute to the decay rate. Representatives of the various classes of graphs are shown in Fig. 5. The classes are (a) irreducible two-loop corrections to the outer vertex; (b) irreducible two-loop corrections to the inner vertex; (c) irreducible two-loop self-energy corrections; (d) reducible two-loop corrections involving one-loop vertex and self-energy parts; (e) ultraviolet and infrared finite generalizations of the double-vertex graph; (f) the double ladder, crossed ladder, and related graphs; (g) one-loop vertex or self-energy corrections to the double-vertex graph; (h) one-loop radiative corrections to the annihilation diagram; (i) vacuum polarization corrections to the one-loop diagrams; (j) the square of the one-loop amplitude; (k) light-by-light scattering of two of the three final state photons. Several of these classes have been calculated earlier: (h) by Adkins and Lymberopoulos [27]; (i) by Burichenko and Ivanov [28] and by Adkins and Shiferaw [29]; and (j) by Burichenko [30] and by Adkins [5]. The rest of the calculations are new. We used dimensional regularization to handle the ultraviolet divergences, and a finite photon mass to regularize all

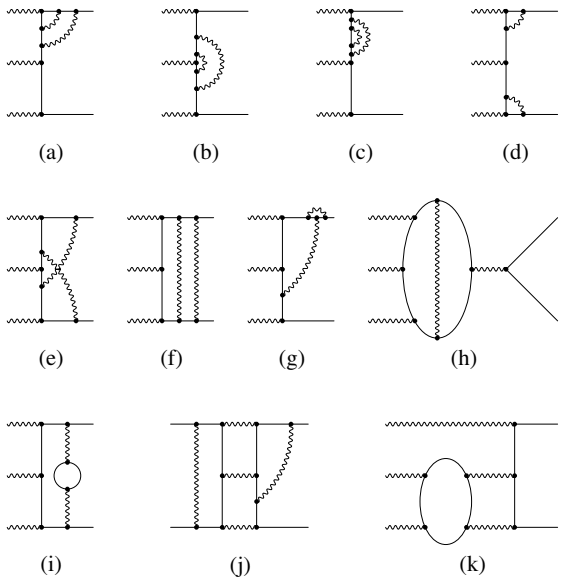

Fig. 5. Two-loop QED graphs contributing to the orthopositronium decay rate. One sample graph is given per class. A spin-one state is implicit on the right. A Cutkosky cut through the three-photon intermediate state to give the imaginary part is implicit in class (j)

infrared divergences. All ultraviolet divergences disappeared after renormalization. The results are listed by class in Table 4 [10]. The complete two-loop QED decay rate result has the form

Table 4. Two-loop QED contributions to the orthopositronium decay rate by class

class	$\frac{\alpha^2}{\lambda^2}\Gamma_0$	$\frac{\alpha^2}{\pi\lambda}\Gamma_0$	$\ln\lambda\frac{\alpha}{\pi}$	$(\frac{\alpha}{\pi})^2\ln^2\lambda\Gamma_0$	$\alpha^2\ln\lambda\Gamma_0$	$(\frac{\alpha}{\pi})^2\Gamma_0$
a	0	0	$-\Gamma_{\rm OV}$	-2	0	-5.618
b	0	0	$-\Gamma_{\rm IV}$	-1	0	-0.705
c	0	0	$-\Gamma_{\rm SE}$	2	0	0.058
d	0	0	0	0	0	2.421
e	0	0	0	0	0	9.259(9)
f	2 ln 2	A	$\Gamma_{\rm SE+OV+IV+DV}$	1	$-\frac{2}{3}$	-20.50(26)
g	0	0	$-\Gamma_{\rm DV}$	0	0	-1.372
h	0	0	0	0	1	9.007
i	0	0	0	0	0	0.965
j	1	A	0	0	0	28.860(2)
k	0	0	0	0	0	0.350(4)[a]
total	2ln 2+1	2A	0	0	$\frac{1}{3}$	22.72(26)

[a] The numerical result for class k is still preliminary.

$$\Gamma_2^{\rm QED} = \big[\frac{(2\ln 2+1)\pi^2}{\lambda^2} + \frac{2\pi A(\lambda)}{\lambda} + \frac{\pi^2}{3}\ln\lambda + B_2\big]\big(\frac{\alpha}{\pi}\big)^2\Gamma_0 \ , \tag{31}$$

where $B_2 = 22.72(26)$.

The appropriate two-loop NRQED graphs are shown in Fig. 6, and the results are given in Table 5. The total two-loop NRQED contribution to the rate is

$$\Gamma_2^{\rm NRQED} = \big[\frac{2\ln 2+1}{\lambda^2} + \big(-\frac{16}{3} - \frac{X}{3}\big)\frac{\Lambda}{\pi\lambda} - \frac{1}{3}\ln\big(\frac{\Lambda}{\lambda}\big) + \frac{2}{3}\ln 2 + \big(-\frac{2}{3} + \frac{5X}{24}\big)\big]\alpha^2\Gamma_0 \ . \tag{32}$$

The two-loop matching condition is

$$\begin{aligned}\Gamma_0 + \Gamma_1^{\rm QED} + \Gamma_2^{\rm QED} &= \big(1 + \frac{\alpha}{\pi}e_1 + \big(\frac{\alpha}{\pi}\big)^2 e_2\big)\Gamma_0 \\ &\quad + \frac{\alpha}{\pi}\Big[\frac{2\pi}{\lambda}\big(1 + \frac{\alpha}{\pi}e_1\big) + \big(-\frac{8}{3} - \frac{X}{6}\big)\Lambda + \big(\frac{7}{12} + \frac{X}{12}\big)\pi\lambda\Big]\Gamma_0 \\ &\quad + \Gamma_2^{\rm NRQED} \ .\end{aligned} \tag{33}$$

The corresponding two-loop coefficient is

$$e_2 = \frac{\pi^2}{3}\ln\Lambda - \frac{\pi^2 X}{24} + \frac{11\pi^2}{6} - \frac{2\pi^2}{3}\ln 2 + B_2 \ . \tag{34}$$

4 The Bound State Calculation

Now that NRQED is defined to the required order, we are in position to obtain the order α^2 correction to the decay rate. The unperturbed problem, defined by

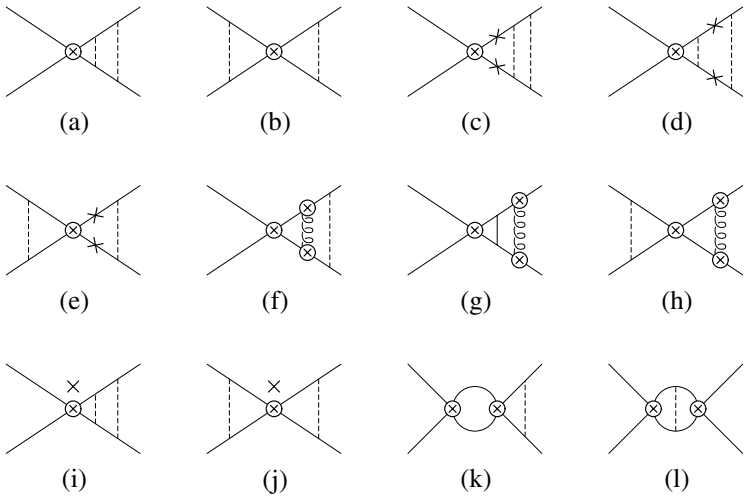

Fig. 6. Two-loop NRQED graphs contributing to the orthopositronium decay rate

Table 5. Two-loop NRQED decay rate contributions

diagram	$\frac{\alpha^2}{\lambda^2}\Gamma_0$	$\frac{\alpha^2\Lambda}{\pi\lambda}\Gamma_0$	$\alpha^2\ln\left(\frac{\Lambda}{\lambda}\right)\Gamma_0$	$\alpha^2\ln 2\Gamma_0$	$\alpha^2\Gamma_0$
a	$2\ln 2$	0	0	0	0
b	1	0	0	0	0
c	0	1	0	0	$-\frac{3}{4}$
d	0	0	$\frac{1}{2}$	$-\frac{1}{2}$	0
e	0	1	0	0	$-\frac{1}{2}$
f	0	$-\frac{5}{3}$	1	$\frac{1}{3}$	$-\frac{5}{8}$
g	0	0	$-\frac{5}{6}$	$\frac{5}{6}$	$\frac{1}{8}$
h	0	$-\frac{5}{3}$	0	0	$\frac{13}{12}$
i	0	$-\frac{X}{6}$	0	0	$\frac{X}{8}$
j	0	$-\frac{X}{6}$	0	0	$\frac{X}{12}$
k	0	-4	0	0	0
l	0	0	-1	0	0
total	$2\ln 2+1$	$-\frac{16}{3}-\frac{X}{3}$	$-\frac{1}{3}$	$\frac{2}{3}$	$-\frac{2}{3}+\frac{5X}{24}$

use of the potential $V_{coul}(\boldsymbol{p},\boldsymbol{q})$, is simply the usual nonrelativistic Schrödinger-Coulomb problem. The ground state wave function has the form

$$\phi(\boldsymbol{p}) = \phi_0 \frac{8\pi\gamma}{(\boldsymbol{p}^2+\gamma^2)^2} \tag{35}$$

where $\gamma = m\alpha/2$ and $\phi_0 = \psi(\boldsymbol{r}=0) = (\gamma^3/\pi)^{1/2}$ is the wave function at contact.

The perturbing potentials are V_4, V_{4der}, δH_{kin}, and V_{BF}. Since we are interested in the imaginary part of the energy shift, at least one factor of a four-point contact term (V_4 or V_{4der}) must be included. Perturbation theory for the ground state energy at second order gives

$$\Delta E = \langle 0|V_4|0\rangle + \langle 0|V_{4der}|0\rangle + \langle 0|V_4\hat{G}V_4|0\rangle + 2\langle 0|V_4\hat{G}\delta H_{kin}|0\rangle + 2\langle 0|V_4\hat{G}V_{BF}|0\rangle \ , \tag{36}$$

where $|0\rangle$ represents the spin-1 ground state, and

$$\hat{G} = \sum_{n\neq 0} \frac{|n\rangle\langle n|}{E_0 - E_n} \tag{37}$$

is the nonrelativistic Schrödinger-Coulomb propagator with the ground state contribution taken out [31,32,33]. The corresponding decay rate contributions are found through use of Eq. 16. After labeling the terms of Eq. 36 as 1-5, we find

$$\Gamma_1 = \big[1 + (\frac{\alpha}{\pi})e_1 + (\frac{\alpha}{\pi})^2 e_2\big]\Gamma_0 \ , \tag{38}$$

$$\Gamma_2 = \big[-\frac{X\alpha}{6\pi}\Lambda + \frac{X\alpha^2}{16}\big]\Gamma_0 \ , \tag{39}$$

$$\Gamma_3 = \big[-\frac{2\alpha}{\pi}\Lambda - \alpha^2\ln(\frac{\Lambda}{\alpha}) - \alpha^2\big]\Gamma_0 \ , \tag{40}$$

$$\Gamma_4 = \big[\frac{\alpha}{\pi}\Lambda + \frac{\alpha^2}{2}\ln(\frac{\Lambda}{\alpha}) + \frac{\alpha^2}{8}\big]\Gamma_0 \ , \tag{41}$$

$$\Gamma_5 = \big[-\frac{5\alpha}{3\pi}\Lambda + \frac{\alpha^2}{6}\ln(\frac{\Lambda}{\alpha}) + \frac{5\alpha^2}{12}\big]\Gamma_0 \ . \tag{42}$$

Ultraviolet divergent integrals were regulated with a momentum cutoff as in the NRQED part of the matching calculation. The total correction to the decay rate is the sum of Eqs. 38 – 42:

$$\Gamma = \big[1 + (\frac{\alpha}{\pi})e_1 + (\frac{\alpha}{\pi})^2 e_2\big]\Gamma_0 + \big[-\frac{8}{3} - \frac{X}{6}\big]\frac{\alpha}{\pi}\Lambda\Gamma_0 + \big[-\frac{1}{3}\ln(\frac{\Lambda}{\alpha}) - \frac{11}{24} + \frac{X}{16}\big]\alpha^2\Gamma_0 \ . \tag{43}$$

Now using the values of e_1 and e_2 (with $\lambda \to 0$), one has

$$\begin{aligned}\Gamma &= \Big\{1 + \frac{\alpha}{\pi}A + (\frac{\alpha}{\pi})^2\big[\frac{\pi^2}{3}\ln\alpha + \pi^2(\frac{11}{8} - \frac{2}{3}\ln 2 + \frac{X}{48}) + B_2\big]\Big\}\Gamma_0 \\ &= \Big\{1 + \frac{\alpha}{\pi}A + (\frac{\alpha}{\pi})^2\big[\frac{\pi^2}{3}\ln\alpha + B_{3\gamma}\big]\Big\}\Gamma_0 \ ,\end{aligned} \tag{44}$$

where

$$B_{3\gamma} = \pi^2\left(\frac{11}{8} - \frac{2}{3}\ln 2 + \frac{X}{48}\right) + B_2 = 44.86(26) \tag{45}$$

is our final result for the three-photon part of the $O(\alpha^2)$ decay rate correction.

References

1. A. Ore and J.L. Powell: Phys. Rev. **75**, 1696 (1949)
2. We used the values $R_\infty = 3.289841960368(25) \times 10^{15}\,Hz$ for the Rydberg constant and $\alpha = 7.297352533(27) \times 10^{-3}$ for the fine structure constant from *The NIST Reference on Constants, Units, and Uncertainty* (http://physics.nist.gov/cuu/; see also P. J. Mohr and B. N. Taylor: *this book*, pp. 145–156). Note that $c = \hbar = 1$ in our units
3. M.A. Stroscio and J.M. Holt: Phys. Rev. A **10**, 749 (1974)
4. W.E. Caswell, G.P. Lepage, and J. Sapirstein: Phys. Rev. Lett. **38**, 488 (1977)
5. G.S. Adkins: Phys. Rev. Lett. **76**, 4903 (1996)
6. W.E. Caswell and G.P. Lepage: Phys. Rev. A **20**, 36 (1979)
7. S.G. Karshenboim: Zh. Eksp. Teor. Fiz. **103**, 1105 (1993) [Sov. Phys. JETP **76**, 541 (1993)]
8. G.S. Adkins and F.R. Brown: Phys. Rev. A **28**, 1164 (1983)
9. G.P. Lepage, P.B. Mackenzie, K.H. Streng, and P.M. Zerwas: Phys. Rev. A **28**, 3090 (1983)
10. G.S. Adkins, R.N. Fell, and J. Sapirstein: Phys. Rev. Lett. **84**, 5086 (2000)
11. R. Hill and G.P. Lepage: hep-ph/0003277
12. B.A. Kniehl and A.A. Penin: hep-ph/0004267
13. K. Melnikov and A. Yelkhovsky: hep-ph/0008099
14. C.I. Westbrook, D.W. Gidley, R.S. Conti, and A. Rich: Phys. Rev. A **40**, 5489 (1989)
15. J.S. Nico, D.W. Gidley, A. Rich, and P.W. Zitzewitz: Phys. Rev. Lett. **65**, 1344 (1990)
16. S. Asai, S. Orito, and N. Shinohara: Phys. Lett. B **357**, 475 (1995)
17. R. S. Conti, R. S. Vallery, D. W. Gidley, J. J. Engbrecht, M. Skalsey, and P. W. Zitzewitz: *this book*, pp. 103–121)
18. W.E. Caswell and G.P. Lepage: Phys. Lett. B **167**, 437 (1986)
19. A.H. Hoang, P. Labelle, and S.M. Zebarjad: Phys. Rev. Lett. **79**, 3387 (1997)
20. A.H. Hoang, P. Labelle, and S.M. Zebarjad: Phys. Rev. A **62**, 012109 (2000)
21. T. Kinoshita and M. Nio: Phys. Rev. D **53**, 4909 (1996)
22. A. Czarnecki, K. Melnikov, and A. Yelkhovsky: Phys. Rev. Lett. **83**, 1135 (1999)
23. A. Czarnecki, K. Melnikov, and A. Yelkhovsky: Phys. Rev. A **61**, 052502 (2000)
24. P. Labelle, G.P. Lepage, and U. Magnea: Phys. Rev. Lett. **72**, 2006 (1994)
25. G.S. Adkins, R.N. Fell, and P.M. Mitrikov: Phys. Rev. Lett. **79**, 3383 (1997)
26. P. Labelle: Ph.D. thesis, Cornell University, 1994
27. G.S. Adkins and M. Lymberopoulos: Phys. Rev. A **51**, 2908 (1995)
28. A.P. Burichenko and D.Y. Ivanov: Yad. Fiz. **58**, 898 (1995) [Phys. At. Nucl. **58**, 832 (1995)]
29. G.S. Adkins and Y. Shiferaw: Phys. Rev. A **52**, 2442 (1995)
30. A.P. Burichenko: Yad. Fiz. **56**, 123 (1993) [Phys. At. Nucl. **56**, 640 (1993)]
31. L. Hostler: J. Math. Phys. **5**, 1235 (1964)
32. J. Schwinger: J. Math. Phys. **5**, 1606 (1964)
33. W.E. Caswell and G.P. Lepage: Phys. Rev. A **18**, 810 (1978)